

Progress in ZnO Materials and Devices

DAVID C. LOOK^{1,2,3}

1.—Semiconductor Research Center, Wright State University, Dayton, OH 45435. 2.—Materials and Manufacturing Directorate, Air Force Research Laboratory, Wright-Patterson Air Force Base, OH 45433. 3.—E-mail address: david.look@wpafb.af.mil

ZnO is a wide-band-gap semiconductor material that is now being developed for many applications, including ultraviolet (UV) light-emitting diodes, UV photodetectors, transparent thin-film transistors, and gas sensors. It can be grown as boules, as thin films, or as nanostructures of many types and shapes. However, as with any useful semiconductor material, its electrical and optical properties are controlled by impurities and defects. Here, we consider various important donor-type impurities, such as H, Al, Ga, and In, and acceptor-type impurities, such as N, P, As, and Sb. We also examine the effects of a few common point defects, including Zn interstitials, Zn vacancies, O vacancies, and complexes of each. The main experimental techniques of interest here include temperature-dependent Hall-effect and low-temperature photoluminescence measurements, because they alone can provide donor and acceptor concentrations and donor energies. The important topic of p-type ZnO is also considered in some detail.

Key words: ZnO, defects, impurities, LEDs, TTFTs

INTRODUCTION

ZnO is an well-known material that has had many applications in such diverse fields as abrasives, brake linings, cosmetics, dental cements, lubricants, paints, phosphors, and rubber products. In fact, these and over fifty other uses of ZnO are described in the 1957 monograph, *Zinc Oxide Rediscovered*, by H.E. Brown.¹ Interestingly, ZnO has been “rediscovered” at least twice since then, in the late 1970s and late 1990s. However, the present rediscovery is the most dramatic, and has generated journal publication rates of well over 1000/yr (for reviews, see Refs. 2–4). One reason for the present resurgence is the recent availability of higher-quality bulk and epitaxial materials, which have enabled the development of ultraviolet (UV) light-emitting diodes (LEDs),^{5–7} transparent thin-film transistors (TTFTs),^{8–10} and nanodevices of many shapes and functions.⁴ Along with the device development, the materials themselves have been studied by a wider variety of sophisticated techniques, and many of the fundamental properties are now more clearly understood. In this paper, we will attempt to summarize the present state of materials knowledge, especially

with regard to the roles of various impurities and defects in controlling the optical and electrical properties. We will also discuss the bottlenecks to further progress, including the development of reliable, robust p-type material. Finally, we will outline some of the recent progress in the development of LEDs, TTFTs, gas sensors, and nanodevices.

IMPURITIES vs. DEFECTS IN ZnO: A HISTORY

As-grown ZnO has always been found to be n-type, and because most samples are grown under Zn-rich conditions, it has been natural in the past to assume that the dominant donor was either the O vacancy (V_O) or the Zn interstitial (Zn_I). This conclusion was strongly challenged, in the year 2000, by Kohan et al.,¹¹ who showed theoretically that both V_O and Zn_I have high formation energies in n-type ZnO and that, furthermore, they are deep, not shallow, donors. They concluded that neither V_O nor Zn_I would exist in measurable quantities, and that even if one or the other were present, its ionization energy would be too high to produce free electrons. Other theoretical analyses have concluded that Zn_I is actually a shallow donor, rather than deep,^{12,13} as has also been shown by electron-irradiation

experiments;¹⁴ however, the high formation energy of Zn_I mentioned earlier would still limit its ability to influence the conductivity of n-type material. Shortly after Kohan et al. showed that V_O and Zn_I were not good explanations for the n-type nature of ZnO, Van de Walle offered an alternative. He argued that H is always a donor in ZnO, that it is easily ionized, and that it has a low enough formation energy to be abundant.¹⁵ This proposal has been subjected to testing, because H-containing, high-quality, bulk ZnO, grown by a seeded chemical vapor transport (SCVT) technique, has been commercially available for the last few years.^{16,17} In general, these tests have confirmed that a shallow donor due to H exists in SCVT ZnO^{18–23} and can contribute significantly to its conductivity. However, some of the Group III elements, such as Al and Ga, are also shallow donors, and are more abundant than H in many cases. Finally, very recent evidence has emerged that even native defects can make important donors, but as complexes, not isolated entities.²⁴ This evidence is not in conflict with the theoretical results of Kohan et al., because their theory deals with isolated defects, not complexes.

EXPERIMENTAL DETAILS

The samples discussed here are $5\text{ mm} \times 5\text{ mm} \times 0.5\text{ mm}$ squares cut from larger wafers that had been sliced from (0001) boules grown by the SCVT method at ZN Technology (Brea, CA).¹⁷ The SCVT technique produces very high quality material. Ohmic In dots were soldered on the corners of the samples, and van der Pauw-Hall effect measurements were performed with a LakeShore Model 7507 apparatus, including a closed-cycle He cooling system operating from 15 K to 320 K. From measurements of Hall coefficient R and conductivity σ , the Hall mobility $\mu_H = R\sigma$ and the Hall concentration $n_H = 1/eR$ could be calculated at each temperature. The true carrier concentration n is related to n_H by $n = rn_H$, where r is the so-called Hall r factor.^{16,25} This r factor was calculated at each temperature, but typically was so close to unity that it was ignored in the plots. Thus, we present only n_H and μ_H data in the plots.

Photoluminescence measurements were performed at 4.2 K. Excitation, dispersion, and detection were accomplished, respectively, with a 45-mW HeCd laser, a 1.25-m spectrometer, and a photomultiplier detector. Resolution was better than 0.01 meV in the spectral range important for this study.

Electron irradiations were carried out at room temperature with a 2-MeV van de Graaff accelerator. A 1.0-MeV beam, of current about $2\ \mu\text{A}/\text{cm}^2$, was directed onto the (0001) Zn-face. Calculations show that a 1-MeV electron beam in the [0001] direction should produce O and Zn displacements at rates of about 0.2 and $0.3\ \text{cm}^{-1}$, respectively.²⁶ Thus, e.g., a fluence of $3 \times 10^{17}\ \text{cm}^{-2}$ would be expected to produce about $6 \times 10^{16}\ \text{cm}^{-3}$ O displacements and $9 \times 10^{16}\ \text{cm}^{-3}$ Zn displacements.

GROUP I IMPURITIES: H AND Li

It has long been known that H always incorporates as a donor in ZnO, even in n-type ZnO,^{1,27} while it is amphoteric in most other semiconductor materials. Van de Walle explained this paradox by showing theoretically that H^- never has a lower formation energy than H^0 or H^+ , so that the donor state is always the preferred state in thermodynamic equilibrium.¹⁵ Subsequent experiments have confirmed this assertion,^{18–23} and, e.g., in Fig. 1, the strongest photoluminescence (PL) feature in the as-grown sample is a donor-bound exciton (D^0, X) line at 3.36258 eV, arising from an exciton bound to interstitial H^0 , and known as I_4 in the literature.²⁸ Note also in Fig. 1 that this line virtually disappears after a series of 0.5-hr anneals at 300–550°C in N_2 gas, because a large share of the H is known to leave the sample at temperatures above 500°C.^{29,30} We obtain further information about the H donor from its two-electron satellite (TES) line near 3.33 eV, designated in Fig. 1 as $I_{4(TES)}$. A TES line occurs when the donor is left in an excited $n = 2$ state upon the collapse of the exciton. From a hydrogenic model, the donor ground state ($n = 1$) energy E_D can then be obtained from $E_D = 4/3(E_{D^0X} - E_{TES})$ giving 44 meV for the H-donor energy.

The concentration of the H donor can be determined by T-Hall measurements, presented in Fig. 2 and 3. The solid lines in these figures are theoretical fits of selected curves using a three-donor model, with the energies of the three donors chosen as 30, 44, and 75 meV. The choice of 44-meV is suggested by the PL-related calculation above for H, and we will show later that a similar analysis yields 30-meV for another important donor. Although the 75-meV donor does not have an obvious PL origin, most of our evidence suggests that it is associated with Al and/or Ga. A summary of the Hall fitting parameters is given in Table I.

The solid lines in Figs. 2 and 3 are fits to the actual experimental data, including the contributions of

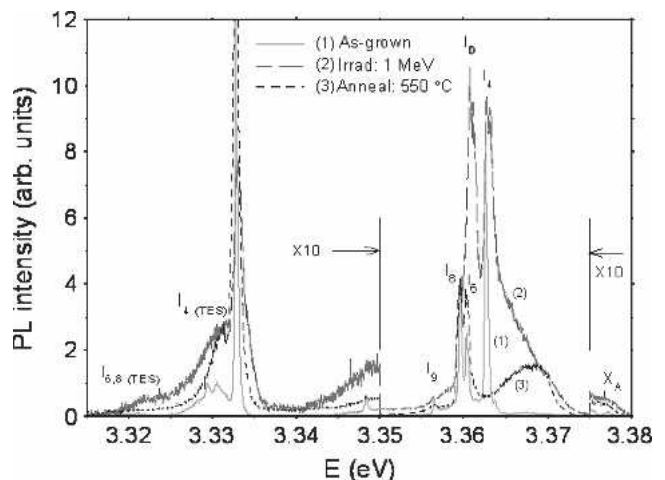


Fig. 1. Photoluminescence at 4 K: (1) as-grown; (2) irradiated with 1-MeV electrons to a fluence of $6 \times 10^{17}\ \text{cm}^{-2}$; and (3) annealed at 550°C for 0.5 hr in flowing N_2 gas.

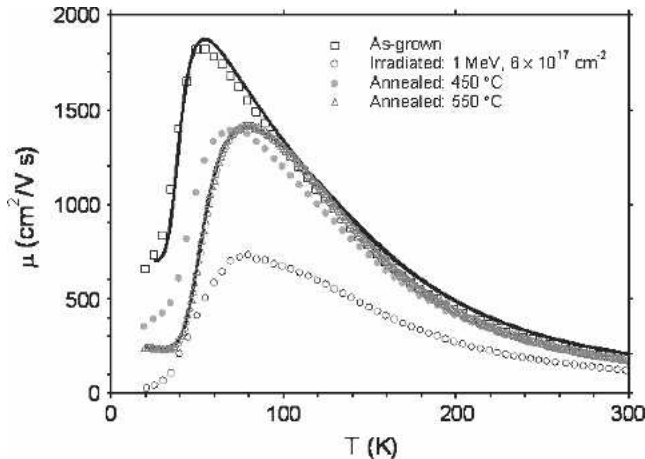


Fig. 2. Mobility vs. temperature: (1) as-grown; (2) irradiated with 1-MeV electrons to a fluence of $6 \times 10^{17} \text{ cm}^{-2}$; (3) annealed at 450°C for 0.5 hr in flowing N_2 gas; and (4) annealed at 550°C . Solid lines are theoretical fits.

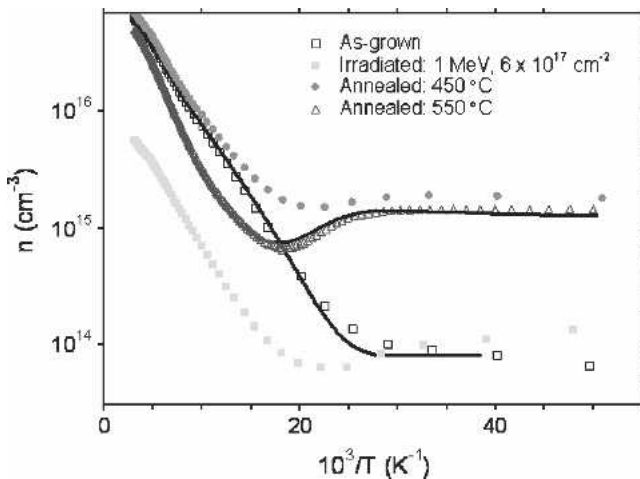


Fig. 3. Carrier concentration vs. temperature: (1) as-grown; (2) irradiated with 1-MeV electrons to a fluence of $6 \times 10^{17} \text{ cm}^{-2}$; (3) annealed at 450°C for 0.5 hr in flowing N_2 gas; and (4) annealed at 550°C . Solid lines are theoretical fits.

surface conduction, which dominates at low temperatures. Surface conduction has been investigated in detail only recently, and probably arises from H adsorbing on the surface from the ambient, or from H diffusing to the surface from the interior of the sample.³¹

From Table I, it is seen that the 44-meV donor (H) concentration drops precipitously as a result of the 550°C anneal. Coupled with the literature studies of H diffusion and effusion as a function of temperature, it is entirely reasonable to assign the 44-meV (T-Hall) and 3.363-eV (PL) fingerprints to H.

Another valence -1 element of high importance is Li. Although theory predicts that Li on the Zn site Li_{Zn} should be a relatively shallow acceptor,^{32,33} it turns out that doping with Li almost always produces semi-insulating (SI) material.^{34,35} The reason evidently involves the fact that the Li interstitial Li_{I} has a lower formation energy than Li_{Zn} in p-type ZnO,

and Li_{I} is a donor. Thus, a sample with high concentrations of Li would attain a balance between Li_{Ga} and Li_{I} and the Fermi level would end up somewhere close to midgap, producing semi-insulating material.

GROUP III ELEMENTS: Al, Ga, AND In

The Group III elements Al, Ga, and In are well-known donor dopants in ZnO, and each can produce carrier concentrations in the $>10^{20} \text{ cm}^{-3}$ range.^{36,37} The PL signatures of Al, Ga, and In are presumably the sharp lines designated I_6 , I_8 , and I_9 , in Fig. 1, occurring in the region of 3.36 eV. Because Al and Ga are often found to be the dominant background impurities in ZnO, and because the 75-meV donor is clearly dominant in our sample, we associate this donor with Al and/or Ga. One potential problem with this association is that the weak lines near 3.32 eV are thought by some to be the TES replicas of I_6 and I_8 , and if so, then the hydrogenic model would give about 55 meV for the Al and Ga donor energies.²⁸ Further research is necessary to resolve this difference in energies.

GROUP IV ELEMENTS: C AND Si

Very little is known of the electrical and optical activity of the Group IV elements, such as C and Si. According to density functional theory (DFT), the split-interstitial complex $(\text{CO})_{\text{O}}$, should be a donor,³⁸ however, its energy is questionable because of the inaccurate DFT treatment of electron correlation, known as the local density approximation (LDA). If N is also present, then the complex $(\text{NC})_{\text{O}}$ is expected to be a shallower donor. Silicon is often present at the $1 \times 10^{16} \text{ cm}^{-3}$ level in SCVT-grown ZnO, according to GDMS analysis;³⁹ however, there is no indication that Si produces shallow levels in the bandgap.

GROUP V ELEMENTS: N, P, As, AND Sb

The elements N, P, As, and Sb, are extremely important for the realization of p-type ZnO. From size considerations, N would seem to be the best choice, and indeed high concentrations ($>10^{20} \text{ cm}^{-3}$) can be achieved. In our SCVT samples, secondary ion mass spectrometry (SIMS) measurements³⁴ show an N concentration of about 10^{17} cm^{-3} , and EPR measurements find that it primarily goes onto the O site, as an acceptor.^{40,41} Interestingly, however, from Table I we see that the total active acceptor concentration in as-grown SCVT samples is only in the low- 10^{15} cm^{-3} range.¹⁶ This is likely because most of the N is passivated with H.^{21,42,43}

Many different growth techniques have been used to produce N-doped ZnO, including chemical vapor deposition (CVD), pulsed laser deposition (PLD), molecular-beam epitaxy (MBE), metalorganic chemical vapor deposition (MOCVD), and rf or dc sputtering.⁴⁴ Moreover, a MBE scheme using temperature modulation has recently been employed to produce good p-type ZnO, and this material has been used to

Table I. Donor and Acceptor Concentrations after Various Treatments

Treatment	N_{D1} (30 meV)	N_{D2} (44 meV)	N_{D3} (75 meV)	N_A
As-grown	0.74	1.7	7.0	0.22
Irradiated: 1 MeV	2.1	0.02	0.3	2.0
Annealed: 450°C	1.2	1.9	7.0	0.36
Annealed: 550°C	0.4	0.1	6.0	0.21

All anneal times were 30 min. Anneals at 300, 350, 400, 450, 500, and 550°C were performed consecutively. The 1-MeV irradiation fluence was $6 \times 10^{17} \text{ cm}^{-2}$. The concentration unit is 10^{16} cm^{-3} .

fabricate homo-epitaxial light-emitting diodes (LEDs).⁷ Some N-doping processes may lead to unstable p-type conductivity,⁴⁵ but most reports of instability are likely due to noisy Hall-effect measurements, or n-type persistent photoconductivity, due to room lights.⁴⁴

In addition to N, also P, As, and Sb can produce good p-type ZnO.^{46–49} To explain this behavior, Limpijumnong et al. have suggested that these larger elements actually go on the Zn site, not the O site, and form a complex, $\text{As}_{\text{Zn}}-2\text{V}_{\text{Zn}}$.⁵⁰ Two recent studies^{51,52} lend credence to this conjecture, although further evidence will be required for verification.

Photoluminescence and T-Hall results on p-type ZnO layers are presented in Figs. 4 and 5, respectively. In Fig. 4, a N-doped layer grown by MBE, and P- and As-doped layers grown by rf sputtering, are compared with a bulk, n-type SCVT sample. It is seen that PL lines at 3.31 eV, 3.357 eV, and 3.367 eV are relatively strong in all of the p-type materials. The 3.31-eV line has been variously conjectured to arise from acceptor-bound excitons, donor-acceptor pairs, or isolated acceptors ($e^- + A^0 \rightarrow A^-$), but at this point, none of these models is certain. The 3.357-eV line is often attributed to In, but another, broader line often appears in the same vicinity after 800°C annealing.⁵³ The 3.367-eV line has been attributed to an ionized donor bound exciton,²⁸ which indeed might be reasonable in p-type material. But

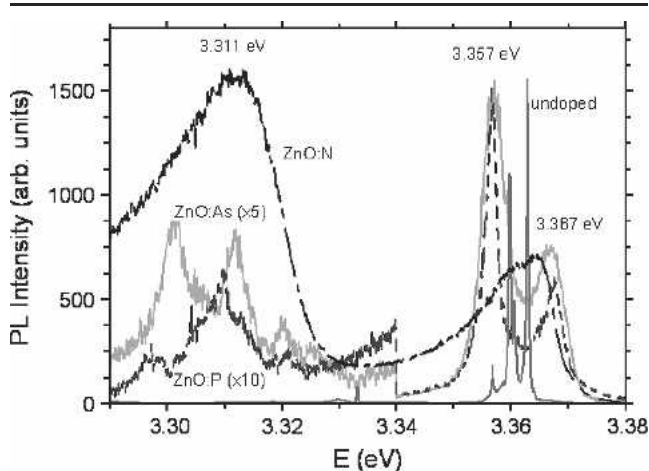


Fig. 4. Comparison of photoluminescence at 4 K for SCVT-grown, undoped, n-type ZnO sample; MBE-grown, N-doped, p-type ZnO layer; rf-sputtered, P-doped, p-type ZnO layer; and rf-sputtered, As-doped, p-type ZnO layer.

at this stage, none of these lines has been unambiguously identified.

The T-Hall results in Fig. 5 involve the As-doped sample shown⁴⁸ in Fig. 4. The 300-K mobility is about $5 \text{ cm}^2/\text{V s}$, a good value for present-day p-type ZnO, and close to what is also usually found in p-type GaN. A simple, one-band fit to the hole-mobility data gives donor and acceptor concentrations in the high- 10^{19}-cm^{-3} range, close to the As concentration found by SIMS. These results are consistent with the p-type nature being due to As acceptors, whether As_O or $\text{As}_{\text{Zn}}-2\text{V}_{\text{Zn}}$. Possible secondary phases, such as As metal or Zn_3As_2 , can also be p-type, but do not seem to be able to explain the data of Fig. 5.

GROUP VII ELEMENTS: F, Cl, Br, AND I

The elements F, Cl, Br, and I should substitute for O and act as donors in ZnO. Indeed, studies have found that F doping greatly decreases the resistivity in ZnO films grown by chemical spray techniques.^{54,55} However, the Group III elements are preferred as donor dopants, and they also seem to be more prevalent as background impurities than the Group VII elements.

DONOR-TYPE POINT DEFECTS

The best way to study point-defect-related donors is to create them by high-energy electron irradiation,^{14,56} and in Fig. 1 we present PL data on a sample irradiated with 1-MeV electrons to a fluence

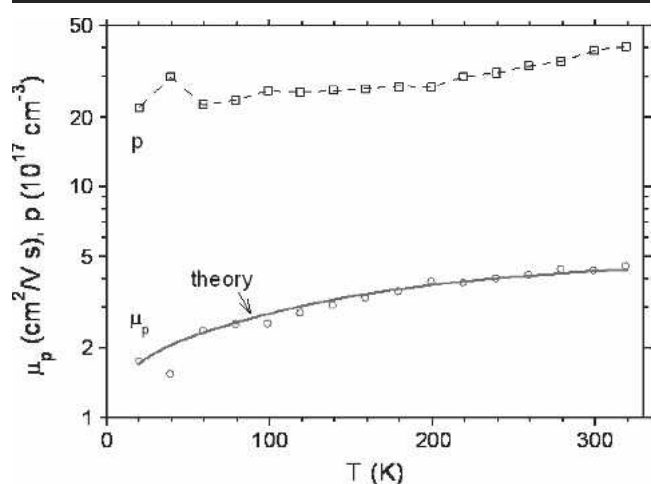


Fig. 5. Mobility and carrier concentration vs. temperature for rf-sputtered, As-doped, p-type ZnO layer.

of $6 \times 10^{17} \text{ cm}^{-2}$. A new D^0 , X line, designated I_D , is produced at 3.3607 eV, and it also has TES lines in the region of 3.338 eV.²⁴ Thus, the defect donor energy is approximately $E_D = 4/3(E_{D^0X} - E_{TES}) = 30 \text{ meV}$. In a separate work, we argue that these lines are associated with a Zn_I complex, probably Zn_I-N_O .²⁴ The changes in mobility and carrier concentration due to the irradiation are shown in Figs. 2 and 3, respectively, and the fits to these curves give the donor and acceptor concentrations shown in Table I. The main results of irradiation are an increase in the 30-meV donor, and decrease in the 75-meV donor. We believe that the increase in the 30-meV donor is due to the creation of Zn interstitials, and the decrease of the 75-meV donor may be due to the complexing of O interstitials (acceptor-like defects) with Group III donors.

The O vacancy produces a deep donor state, according to theory.^{11–13} In agreement, EPR experiments have seen deep states associated with V_O .⁵⁷ On the other hand, positron annihilation spectroscopy suggests that a shallow (~ 100 -meV) V_O -related state may also exist.⁵⁸ Thus, more research on this matter is needed.

Besides Zn_I and V_O , the antisite Zn_O should also be a donor, although there is some disagreement among theoreticians on whether it is shallow or deep.^{11–13} In any case, right now there is little strong evidence for any optical or electrical activity due to Zn_O .

ACCEPTOR-TYPE POINT DEFECTS

According to theory, the O interstitial O_I and Zn vacancy V_{Zn} should behave as acceptors,^{11–13} and V_{Zn} , at least, should be prevalent in n-type ZnO, especially in material created under O-rich conditions. Experimentally, little is known about O_I , which can exist in both tetrahedral and octahedral positions. However, much is known about V_{Zn} , because as a negatively charged vacancy, it can easily trap positrons. In fact, the small acceptor concentration of $(1-2) \times 10^{15} \text{ cm}^{-3}$ in as-grown SCVT ZnO (Table I) can be entirely explained by V_{Zn} -related defects.⁵⁹ As mentioned before, there are also N_O -related acceptors in SCVT ZnO, but they are likely neutralized by H unless the sample has been subjected to annealing or irradiation.^{21,42,43}

APPLICATIONS

As mentioned earlier, ZnO has long been a key ingredient in various products such as lubricants, paints, and phosphors.¹ However, the recent revival of interest in this material is more concerned with electronic and photonic applications. Here we will mention only four of them: (1) UV LEDs; (2) UV photodetectors (PDs); (3) transparent thin-film transistors (TTFTs); and (4) gas sensors. Also, we will consider one recent application of each, rather than try to survey the whole field. Reviews of earlier work can be found in Refs. 1–4.

1. Examples of LEDs involving ZnO are given in Refs. 5–7. Reference 7 describes a homo-epitaxial LED, whereas Refs. 5 and 6 deal with hetero-epitaxial structures. In Ref. 6, Osinsky et al. discuss a p–n junction LED with the p-layer being Mg-doped $Al_{0.16}Ga_{0.84}N$ ($p \sim 1 \times 10^{17} \text{ cm}^{-3}$), and the n-layer, Ga-doped ZnO ($n \sim 3 \times 10^{17} \text{ cm}^{-3}$). The junction I–V curve has a turn-on voltage of about 3.2–3.6 eV, which is consistent with the ZnO bandgap, and the reverse breakdown voltage is $\sim 15 \text{ V}$. The electroluminescence (EL) peak energy is $\sim 390 \text{ nm}$ at 300 K, with a 40-nm FWHM, and the peak energy increases to 391 nm at 500-K operation, with a FWHM of only 28 nm. About 40% of the 300-K EL intensity is maintained even at 650 K, showing the strong advantages of ZnO at high temperatures. The EL spectrum is very similar to the PL spectrum of the ZnO layer by itself, proving that the electron-hole recombinations are occurring in the ZnO and are excitonic in nature. Although the UV optical power is very weak in this prototype device, only about 10 μW at 300 K, it should improve significantly with optimization of the structure.
2. An example of a UV metal–semiconductor–metal (MSM) photodetector based on ZnO is given in Ref. 60. This device is based on a 1- μm -thick, N-doped ZnO layer grown by MOCVD on R-plane sapphire. Here, N doping is introduced to increase the resistivity of the n-type ZnO by adding acceptor compensation. The cutoff wavelength of this detector is 373 nm, and the photoresponsivity is very high, 400 A/W at 5-V bias, fairly flat from about 285 nm to the cutoff. The time response is also good, with rise and fall times of about 1 μs .
3. Some recent works on TTFTs are described in Refs. 8–10. Such devices are used extensively in the electronic flat-panel display industry, and at present are based on amorphous Si (α -Si), or polycrystalline Si (poly-Si). Each of these materials has severe limitations: α -Si is light-sensitive, degrades in strong light, and has a low mobility ($< 2 \text{ cm}^2/\text{V s}$); and poly Si, while having a high mobility ($\sim 50 \text{ cm}^2/\text{V s}$), is opaque. Furthermore, each of these materials is grown at temperatures well above room temperature, and thus cannot be integrated with organic LEDs or polymer-based flexible substrates. On the other hand, ZnO TTFTs, fabricated at room temperature, can overcome all of these problems. The structure discussed in Ref. 10 uses indium tin oxide (ITO) for the gate, a superlattice of Al_2O_3 and TiO_2 (ATO) for the gate dielectric, and Ga-doped ZnO for the source and drain regions. This device has a high saturation mobility of $20 \text{ cm}^2/\text{V s}$, a threshold voltage of 21 V, a gate-voltage swing of 1.24 V/decade, and an on/off ratio of 2×10^5 . Furthermore, the average transmission in the visible part of the spectrum is about 80%, and most of the 20% loss is due to

the uncoated glass substrate, not the ZnO TFT. Clearly, ZnO-based TFTs are far superior in many ways to their Si counterparts.

4. Different types of semiconductor nanostructures are now being developed for many applications. One of the most popular nanostructure materials is ZnO, because it can be grown by many different techniques and at low temperatures. Furthermore, its wurtzite structure is ideal for the growth of nanowires or nanorods, with a c-axis orientation. Finally, its reactive surface lends itself to gas-sensing applications. A recently reported ZnO-based gas sensor for H₂ consists of MBE-grown, Pd-coated nanorods with diameters of 30–150 nm, and lengths of 2–10 μm.⁶¹ Exposure to 10 ppm of H₂ in N₂ gas changes the resistance of the nanorods by about 3%, an easily measurable change with a signal/noise ratio > 10. This device can be reset to its initial state by exposure to air for ~20 s. Many other applications of ZnO nanostructures can be found in Ref. 4.

SUMMARY

Temperature-dependent Hall-effect and low-temperature photoluminescence measurements have been carried out on as-grown, annealed, and electron-irradiated ZnO samples and have yielded the energies and concentrations of several donors and acceptors. The primary donors in SCVT-grown n-type material are H, Al, Ga, and a Zn-interstitial complex, while the primary acceptor is the Zn vacancy. For doping purposes, Al and Ga are usually chosen as donors, and N, P, and As, as acceptors. Still, however, high-conductivity p-type material is difficult to grow reproducibly, and this problem must be overcome to permit strong advances in the LED industry. Other applications that have bright futures include UV detectors, transparent thin-film transistors, and nanostructures of many kinds.

ACKNOWLEDGEMENTS

We thank T.A Cooper and W. Rice for technical assistance and B.B. Claffin and C.W. Litton for helpful discussions. Support was provided by the U.S. Air Force (contract F33615-00-C-5402) and sub-contracts with Structured Materials Industries, Inc., and with SVTA, Inc. Much of the work was performed at the Air Force Research Laboratory, Wright-Patterson AFB, Ohio.

REFERENCES

1. H.E. Brown, *ZnO Rediscovered* (New York: The New Jersey Zinc Co., 1957), p. 31.
2. D.C. Look, *Mater. Sci. Eng.*, B 80, 383 (2001).
3. S.J. Pearton, D.P. Norton, K. Ip, Y.W. Heo, and T. Steiner, *Prog. Mater. Sci.* 50, 293 (2005).
4. G.-C. Yi, C. Wang, and W.I. Park, *Semicond. Sci. Technol.* 20, S22 (2005).
5. Ya.I. Alivov, E.V. Kalinina, A.E. Cherenkov, D.C. Look, B.M. Ataev, A.K. Omaev, M.V. Chukichev, and D.M. Bagnall, *Appl. Phys. Lett.* 83, 4719 (2003).
6. A. Osinsky, J.W. Dong, M.Z. Kauser, B. Hertog, A.M. Dabiran, P.P. Chow, S.J. Pearton, O. Lopatiuk, and L. Chernyak, *Appl. Phys. Lett.* 85, 4272 (2004).
7. A. Tsukazaki et al., *Nat. Mater.* 4, 42 (2005).
8. J.F. Wager, *Science* 300, 1245 (2003).
9. R.L. Hoffman, *J. Appl. Phys.* 95, 5813 (2004).
10. E.M.C. Fortunato, P.M.C. Barquinha, A.C.M.P.G. Pimental, A.M.F. Gonçalves, A.J.S. Marques, L.M.N. Pereira, and R.F.P. Martins, *Adv. Mater.* 17, 590 (2005).
11. A.F. Kohan, G. Ceder, D. Morgan, and C.G. Van de Walle, *Phys. Rev. B: Condens. Matter Mater. Phys.* 61, 15019 (2000).
12. S.B. Zhang, S.-H. Wei, and A. Zunger, *Phys. Rev. B: Condens. Matter Mater. Phys.* 63, 075205 (2001).
13. F. Oba, S.R. Nishitani, S. Isotani, H. Adachi, and I. Tanaka, *J. Appl. Phys.* 90, 824 (2001).
14. D.C. Look and J.R. Sizelove, *Phys. Rev. Lett.* 82, 2552 (1999).
15. C.G. Van de Walle, *Phys. Rev. Lett.* 85, 1012 (2000).
16. D.C. Look, D.C. Reynolds, J.R. Sizelove, R.L. Jones, C.W. Litton, G. Cantwell, and W.C. Harsch, *Solid State Commun.* 105, 399 (1998).
17. ZN Technology, 910 Columbia Street, Brea, CA 92821.
18. S.F.J. Cox et al., *Phys. Rev. Lett.* 86, 2601 (2001).
19. D.M. Hofmann, A. Hofstaetter, F. Leiter, H.J. Zhou, F. Henecker, B.K. Meyer, S.B. Orlinskii, J. Schmidt, and P.G. Baranov, *Phys. Rev. Lett.* 88, 045504 (2001).
20. K. Shimomura, K. Nishiyama, and R. Kadono, *Phys. Rev. Lett.* 89, 255505 (2002).
21. N.H. Nickel and K. Fleischer, *Phys. Rev. Lett.* 90, 197402 (2003).
22. K. Ip, M.E. Overberg, Y.W. Heo, D.P. Norton, S.J. Pearton, C.E. Stutz, B. Luo, F. Ren, D.C. Look, and J.M. Zavada, *Appl. Phys. Lett.* 82, 385 (2003).
23. Y.M. Strzhemechny, H.L. Mosbacker, D.C. Look, D.C. Reynolds, C.W. Litton, N.Y. Garces, N.C. Giles, L.E. Halliburton, S. Niki, and L.J. Brillson, *Appl. Phys. Lett.* 84, 2545 (2004).
24. D.C. Look, G.C. Farlow, S. Limpijumnong, S.B. Zhang, and K. Nordlund, *Phys. Rev. Lett.* 95, 225502 (2005).
25. D.C. Look, *Electrical Characterization of GaAs Materials and Devices* (New York: Wiley, 1989), Chap. 1.
26. P. Erhart, K. Albe, N. Juslin, and K. Nordlund, unpublished.
27. Y.-S. Kang, H.-Y. Kim, and J.-Y. Lee, *J. Electrochem. Soc.* 147, 4625 (2000).
28. B.K. Meyer, H. Alves, D.M. Hofmann, W. Kriegseis, D. Forster, F. Bertram, J. Christen, A. Hoffmann, M. Strassburg, M. Dworzak, U. Haboek, and A.V. Rodina, *Phys. Status Solidi* 241b, 231 (2004).
29. N.H. Nickel and K. Fleischer, *Phys. Rev. Lett.* 90, 197402 (2003).
30. D.C. Look, R.L. Jones, J.R. Sizelove, N.Y. Garces, N.C. Giles, and L.E. Halliburton, *Phys. Status Solidi* 195a, 171 (2003).
31. D.C. Look, H.L. Mosbacker, Y.M. Strzhemechny, and L.J. Brillson, *Superlattices and Microstructures* 38, 406 (2005).
32. C.H. Park, S.B. Zhang, and S.H. Wei, *Phys. Rev. B: Condens. Matter Mater. Phys.* 66, 073202 (2002).
33. M.G. Wardle, J.P. Goss, and P.R. Briddon, *Phys. Rev. B: Condens. Matter Mater. Phys.* 71, 155205 (2005).
34. D.C. Look, D.C. Reynolds, C.W. Litton, R.L. Jones, D.B. Eason, and G. Cantwell, *Appl. Phys. Lett.* 81, 1830 (2002).
35. X.S. Wang, Z.C. Wu, J.F. Webb, and Z.G. Liu, *Appl. Phys. A* 77, 561 (2003).
36. K.-K. Kim, S. Niki, J.-Y. Oh, J.-O. Song, T.-Y. Seong, S.-J. Park, S. Fujita, and S.-W. Kim, *J. Appl. Phys.* 97, 066013 (2005).
37. T. Makino, Y. Segawa, S. Yoshida, A. Tsukazaki, A. Ohtomo, and M. Kawasaki, *Appl. Phys. Lett.* 85, 759 (2004).
38. S. Limpijumnong, X. Li, S.-H. Wei, and S.B. Zhang, *Appl. Phys. Lett.* 86, 211910 (2005).
39. G. Cantwell and Z.N. Technology, private communication.
40. W.E. Carlos, E.R. Glaser, and D.C. Look, *Phys. B* 308-310, 976 (2001).
41. N.Y. Garces, N.C. Giles, L.E. Halliburton, G. Cantwell, D.B. Eason, D.C. Reynolds, and D.C. Look, *Appl. Phys. Lett.* 80, 1334 (2002).

42. C.H. Seager and S.M. Myers, *J. Appl. Phys.* 94, 2888 (2003).
43. L.E. Halliburton, L. Wang, L. Bai, N.Y. Garces, N.C. Giles, M.J. Callahan, and B. Wang, *J. Appl. Phys.* 96, 7168 (2004).
44. D.C. Look, B. Clafin, Ya.I. Alivov, and S.J. Park, *Phys. Status Solidi a* 201, 2203 (2004).
45. T.M. Barnes, K. Olson, and C.A. Wolden, *Appl. Phys. Lett.* 86, 112112 (2005).
46. Y.R. Ryu, S. Zhu, D.C. Look, J.M. Wrobel, H.M. Jeong, and H.W. White, *J. Cryst. Growth* 216, 330 (2000).
47. K.-K. Kim, H.-S. Kim, D.-K. Hwang, J.-H. Lim, and S.-J. Park, *Appl. Phys. Lett.* 83, 63 (2003).
48. D.C. Look, G.M. Renlund, R.H. Burgener II, and J.R. Sizelove, *Appl. Phys. Lett.* 85, 5269 (2004).
49. F.X. Xiu, Z. Yang, L.J. Mandalapu, D.T. Zhao, and J.L. Liu, *Appl. Phys. Lett.* 87, 152101 (2005).
50. S. Limpijumnong, S.B. Zhang, S.-H. Wei, and C.H. Park, *Phys. Rev. Lett.* 92, 155504 (2004).
51. U. Wahl, E. Rita, J.G. Groves, A.C. Marques, E. Alves, and J.C. Soares, *Phys. Rev. Lett* 95, 215503 (2005) .
52. F. Tuomisto, I. Makkonen, M.J. Puska, K. Saarinen, D.C. Look, G.M. Renlund, and R.H. Burgener II, *Superlattices Microstruct.* in press.
53. D.C. Reynolds, D.C. Look, B. Jogai, C.W. Litton, T.C. Collins, W. Harsch, and G. Cantwell, *Phys. Rev. B: Condens. Matter Mater. Phys.* 57, 12151 (1998).
54. A. Guillén-Santiago, M. de la L. Olvera, A. Maldonado, R. Asomoza, and D.R. Acosta, *Phys. Status Solidi a* 201, 952 (2004).
55. P.M. Ratheesh Kumar, C. Sudha Kartha, K.P. Vijayakumar, F. Singh, and D.K. Avasthi, *Mater. Sci. Eng., B* 117, 307 (2005).
56. D.C. Look, D.C. Reynolds, J.W. Hensky, R.L. Jones, and J.R. Sizelove, *Appl. Phys. Lett.* 75, 811 (1999).
57. P. Kasai, *Phys. Rev.* 130, 989 (1963).
58. F. Tuomisto, K. Saarinen, D.C. Look, and G.C. Farlow, *Phys. Rev. B: Condens. Matter Mater. Phys.* 72, 085206 (2005).
59. F. Tuomisto, K. Saarinen, and D.C. Look, *Phys. Rev. Lett.* 91, 205502 (2003).
60. Y. Liu, C.R. Gorla, S. Liang, N. Emanetoglu, Y. Lu, H. Shen, and M. Wraback, *J. Electron. Mater.* 29, 69 (2000).
61. H.T. Wang, B.S. Kang, F. Ren, L.C. Tien, P.W. Sadik, D.P. Norton, S.J. Pearton, and J. Lin, *Appl. Phys. Lett.* 86, 243503 (2005).